VILNIUS UNIVERSITY

Aušrinė
NESTARENKAITĖ

Immune response assessment in a colorectal cancer microenvironment using digital pathology analytics

SUMMARY OF DOCTORAL DISSERTATION

Natural Sciences,
Biology (N 010)

VILNIUS 2021

This dissertation was written during 2015–2020 at the National Center of Pathology, Affiliate of Vilnius University Hospital Santaros Klinikos, and at the Institute of Biosciences, Life Sciences Center, Vilnius University.

Academic supervisor – Dr. Aida Laurinavičienė (Vilnius University, Medicine and Health Sciences, Medicine, M 001).
Academic consultant – Prof. Dr. Sonata Jarmalaitė (Vilnius University, Natural Sciences, Biology, N 010). During 2015-10-01 and 2019-06-18.

This doctoral dissertation will be defended in a public meeting of the Dissertation Defence Panel:
Chairman – Prof. Dr. Jolanta Gulbinovič (Vilnius University, Medicine and Health Sciences, Medicine, M 001).
Members:
Dr. Audrius Dulskas (National Cancer Institute, Medicine and Health Sciences, Medicine, M 001);
Dr. Jonathan A. Nowak (Harvard Medical School, Natural Sciences, Biology, N 010);
Prof. Habil. Dr. Dalia Pangonytė (Lithuanian University of Health Sciences, Natural Sciences, Biology, N 010);
Dr. Vita Pašukonienė (National Cancer Institute, Natural Sciences, Biology, N 010).

The dissertation shall be defended at a public meeting of the Dissertation Defence Panel on 1st of July 2021, at 13 p.m., at Life Sciences Center, Vilnius University. Address: Sauletekio Ave. 7 (auditorium R-401), LT-10257, Vilnius, Lithuania.

The doctoral dissertation is available for review at the Library of Vilnius University and Vilnius University website:
https://www.vu.lt/lt/naujienos/ivykiu-kalendorius

VILNIAUS UNIVERSITETAS

Aušrinė
NESTARENKAITĖ

Imuninio atsako storosios žarnos vėžio mikroaplinkoje vertinimas skaitmeninės patologijos analitikos metodais

DAKTARO DISERTACIJOS SANTRAUKA

Gamtos mokslai,
Biologija (N 010)

VILNIUS 2021

Disertacija rengta 2015–2020 metais Valstybiniame patologijos centre, Vilniaus universiteto ligoninės Santaros klinikų filiale, ir Biomokslų institute, Gyvybės mokslų centre, Vilniaus universitete.

Mokslinė vadovė – dr. Aida Laurinavičienė (Vilniaus universitetas, medicinos ir sveikatos mokslai, medicina, M 001)
Mokslinė konsultantė – prof. dr. Sonata Jarmalaitė (Vilniaus universitetas, gamtos mokslai, biologija, N 010). Nuo 2015-10-01 iki 2019-06-18

Gynimo taryba:
Pirmininkė – prof. dr. Jolanta Gulbinovič (Vilniaus universitetas, medicinos ir sveikatos mokslai, medicina, M 001)
Nariai:
dr. Audrius Dulskas (Nacionalinis vėžio institutas, medicinos ir sveikatos mokslai, medicina, M 001)
dr. Jonathan A. Nowak (Harvardo medicinos mokykla, gamtos mokslai, biologija, N 010)
prof. habil. dr. Dalia Pangonytė (Lietuvos sveikatos mokslų universitetas, gamtos mokslai, biologija, N 010)
dr. Vita Pašukonienė (Nacionalinis vėžio institutas, gamtos mokslai, biologija, N 010)

Disertacija ginama viešame Gynimo tarybos posėdyje 2021 m. liepos mėn. 1 d. 13 val. Vilniaus universiteto Gyvybės mokslų centre, R-401 auditorijoje (Saulėtekio al. 7, LT-10257, Vilnius, Lietuva) ir/arba nuotoliniu būdu.

Disertaciją galima peržiūrėti Vilniaus universiteto bibliotekoje ir VU interneto svetainėje adresu:
https://www.vu.lt/lt/naujienos/ivykiu-kalendorius

ABBREVIATIONS

BRAF	– v-Raf murine sarcoma viral oncogene homolog B; proto-oncogene, serine/threonine kinase
CI	– confidence interval
CM	– Center of Mass
CRC	– colorectal cancer
DIA	– digital image analysis
EGFR	– epidermal growth factor receptor
FFPE	– formalin-fixed paraffin-embedded
HR	– hazard ratio
ID	– Immunodrop
IHC	– immunohistochemistry
IZ	– tumor-stroma interface zone
KRAS	– Kirsten rat sarcoma viral oncogene homolog; proto-oncogene, GTPase
LR	– likelihood ratio
MEK	– mitogen-activated protein kinase kinase
MSI	– microsatellite instability
MSS	– microsatellite stability
NRAS	– neuroblastoma RAS viral oncogene homolog; proto-oncogene, GTPase
OS	– overall survival
PIK3CA	– phosphatidylinositol -4,5-bisphosphate 3-kinase catalytic subunit alpha
TE	– tumor edge
TIL	– tumor infiltrating lymphocyte
TME	– tumor microenvironment
TNM	– tumor-node-metastasis staging system
WSI	– whole slide image

INTRODUCTION

Colorectal cancer (CRC) is one of the most common cancers and one of the leading causes of cancer-related deaths worldwide. Advancements in the diagnostics and personalized treatment of cancer prolong patient survival (Bray F. *et al.*, 2018). However, the biology of CRC is highly multifaceted; therefore, even in cases of similar clinical and pathological features, there is variation in the outcomes of patients (Molinari C. *et al.*, 2018).

The tumor-node-metastasis (TNM) classification of malignant tumors is a standard for staging the extent of cancer spread and predicting the disease course (Brierley J. *et al.*, 2017). Tumor localization (Baran B. *et al.*, 2018), as well as the histological grade and budding, are taken into account for planning the treatment of CRC; however, the assessment of the latter criteria is difficult to standardize (Barresi V. *et al.*, 2015; Lugli A. *et al.*, 2016.). In general, histopathological tumor characteristics are insufficiently informative prognostic and predictive markers; thus, additional tumor molecular and microenvironment markers are used to achieve a more accurate classification of CRC (Park J. *et al.*, 2015; Dienstmann R. *et al.*, 2017).

The clinically relevant CRC markers are limited in part due to the high genetic heterogeneity inherent for this type of cancer (Zhai Z. *et al.*, 2017). Currently, the CRC diagnostics involves only a few molecular markers (Giardiello F. *et al.*, 2014; Van Cutsem E. *et al.*, 2016; Provenzale D. *et al.*, 2018): *KRAS* and *NRAS* gene mutations are predictive markers for anti-EGFR therapy resistance in metastatic CRC; microsatellite instability (MSI) is tested for Lynch syndrome diagnostics and is a predictive marker for adjuvant chemotherapy resistance in stage II CRC and of a favourable response for immunotherapy in metastatic CRC; *BRAF* gene mutations have been associated with a more aggressive course of the disease, and *BRAF*-mutated metastatic CRC was reported to be responsive to the combined BRAF, MEK inhibitors and anti-EGFR therapy (Kopetz S. *et al.*, 2020). Several gene expression profiling panels, such as

Onco*type* DX®, ColoPrint®, ColDx®, have been developed to assess the risk of relapse in stage II CRC, but their use is not currently recommended due to insufficient data to support the added clinical and predictive value (Sharif S. *et al*., 2012; Provenzale D. *et al.* 2018).

Extensive research in the past few decades has revealed that the tumor microenvironment (TME) has a significant impact on cancer pathogenesis and progression (Hanahan D. *et al.,* 2012). One of the most clinically relevant features of TME is a local antitumor immune response (Turley S. *et al*., 2015; Labani-Motlagh A. *et al.,* 2020). High cytotoxic and memory tumor infiltrating lymphocyte (TIL) densities correlate with a lower risk of cancer progression and a favourable response to immune checkpoint inhibitors in various cancers (Pages F. *et al.*, 2009; Hendry S. *et al.*, 2017; Hou Y. *et al.*, 2018; Plesca I. *et al.*, 2020). CRC research has revealed the heterogeneity of TIL distribution in TME and thus the importance of the immune contexture, i.e., the effectiveness of antitumor immune response depends not only on TIL subtypes and absolute densities, but also on their spatial distribution in the tissue (Galon J. *et al*., 2007). These trends were later observed in melanoma, breast, and lung cancer (Yuan Y. *et al.*, 2015; Corredor G. *et al.* 2019; Bosisio F. *et al.*, 2020). Also, CRC with MSI, which causes tumor immunogenecity and a rich immune infiltrate (Kloor M. *et al.*, 2016), are associated with prolonged patient survival (Marcus L. *et al.*, 2019; Luchini C. *et al.*, 2019). In 2020, the American Food and Drug Administration approved the programmed cell death protein 1 (PD-1)-targeted immunotherapy for the first line treatment of patients with MSI metastatic CRC; however, about 60% of the patients treated did not respond to the therapy (Asaoka Y. *et al.*, 2015; Andre T. *et al.*, 2020). Recent data reveal significant intertumoral heterogeneity in TIL densities among CRCs with MSI and that 26–35% of these tumors do not exhibit a rich immune infiltrate (Yoon H. *et al.*, 2019). Thus, the variance of TIL densities partly explains the insufficient prognostic/predictive power of the MSI marker and directs us towards immune contexture studies.

Different methods are employed for the extraction of optimal immune response indicators that could predict cancer progression. More accurate and precise quantitative measurements of *in situ* immune infiltrate are achieved by digital image analysis (DIA). Spatial analytics further increase the power of the TME immune contexture studies to obtain an added prognostic value. In 2012, Galon *et al.* proposed the Immunoscore® methodology for CRC, which is based on digital immunohistochemistry (IHC) and designed for the quantification of total and cytotoxic T lymphocyte densities in the core tumor and the invasive margin (Galon J. *et al.*, 2012). In 2018, Immunoscore® was validated as an independent prognostic factor that outperformed conventional cancer markers, including TNM criteria and MSI status (Mlecnik B. *et al.*, 2016; Pages F. *et al.*, 2018). Recently, Nearchou *et al.* proposed a spatial immuno-oncology index which combines TIL and macrophage subpopulation densities in the core tumor and ivasive margin regions as well as TIL density in a 50 µm radius around tumor buds in the periphery of invasive margin; this index was an independent prognostic factor and stratified patients in three independent stage II CRC patient cohorts (Nearchou I. et *al.*, 2019 and 2020). Lazarus *et al.* performed the analysis of the metastatic CRC microenvironment and revealed that high cytotoxic T lymphocyte density in a 15 µm radius around tumor cells was an independent predictor of longer patient survival (Lazarus J. *et al.*, 2018). Similarly, high cytotoxic T lymphocyte and programmed death ligand 1 (PD-L1) positive immune cell densities within 20 µm to tumor cells were markers of response to anti-PD-1 therapy in metastatic melanoma (Gide T. *et al.*, 2020). In general, currently developed immune response profiling systems emphasize the additional prognostic information provided by the analysis of immune and tumor cell spatial interactions (Enfield K. *et al.* 2019; Pang S. *et al.*, 2019). Recently, combined models that integrate tumor histopathological or molecular features and immune contexture indicators have shown improved prognostic power in CRC and other cancers (Nearchou I. *et al.,* 2019 and 2020).

Scientific relevance and novelty

In this study we searched for DIA and spatial analytics methods to extract informative immune response indicators that would provide independent prognostic value in the CRC patient cohorts. By combining DIA, artificial intelligence tools, and hexagonal grid analytics with a unique set of explicit rules, we came up with a methodology that provides novel type indicators based on TIL density profiles across the tumor-stroma interface zone (IZ). In particular, the methodology 1) utilizes spatial analytics methods to automatically detect and rank the IZ between the tumor epithelium and the surrounding stroma, 2) extracts the absolute TIL density and its directional change (Immunogradient) towards the tumor in the IZ, 3) provides combined IZ Immunogradient-based scores as strong independent prognostic factors for CRC patients.

Other immune response profiling methodologies are based on absolute TIL densities measured in the core tumor and invasive margin regions (Pages F. *et al.*, 2018), but do not assess the directional TIL density profiles within the proper interface between the tumor epithelium and the surrounding stroma. In addition, most methodologies utilize a fixed-width invasive margin, which introduces a potential bias due to a variable and frequently irregular tumor growth pattern. In contrast, the IZ concept and method rely on a probability of a specific TME location to represent the tumor edge (TE) and the IZ ranks towards tumor or stroma compartments. This detection is based on explicit rules and allows variable IZ width adaptable to the spatial diversity of the tumor. The IZ and immune response indicators are based on high capacity and automated computational procedures, therefore, are independent of visual assessment by an expert and, in fact, often represent subvisual features that cannot be quantified using routine microscopy. IZ can be optimized for the analysis of various immune infiltrates in different pathology or non-pathology tissues.

We explored the prognostic power of the proposed immune response indicators in two independent CRC patient cohorts from

Vilnius and Nottingham health care institutions: cytotoxic T cell (CD8) Immunogradient in both cohorts, in addition, B cell (CD20) Immunogradient and histological tumor growth pattern, in Nottingham cohort, revealed an independent prognostic value in patient overall survival predictions. CD8 and CD20 Immunogradients outperformed absolute immune cell densities in the TME and conventional clinicopathological and molecular markers. We generated novel combined models to predict overall patient survival: CD8-CD20 Immunogradient score based only on CD8 and CD20 IHC markers, and Immuno-interface score that also integrates histological tumor growth pattern. The prognostic power of these scores was superior to tumor TNM classification criteria and MSI status which are still considered to be the key markers in predicting the clinical course and response to cytotoxic chemotherapy and immunotherapy in CRC.

The aim and objectives of the study

The aim of this study was to develop an automated quantitative system based on digital image analysis for the assessment of immune response in the tumour microenvironment and evaluate its prognostic power in colorectal cancer patients.

The objectives of the study:

1. To develop a methodology based on digital image analysis and spatial statistics for the profiling of immune cell distributions in the tumour microenvironmet, and to select informative quantitative indicators for the assessment of the immune response in the colorectal cancer microenvironment.
2. To determine the prognostic value of the immune response indicators in two independent colorectal cancer patient cohorts.
3. To generate combined prognostic models for colorectal cancer and evaluate their power in relation to conventional clinicopathological and molecular markers.

Statements to be defended

1. TIL assessed by Immunogradient indicators in the tumor-stroma IZ are independent prognostic factors of overall CRC patient survival and are more informative than absolute TIL densities in the TME or conventional clinicopathological and molecular markers.
2. Combined CD8-CD20 Immunogradient and immuno-interface scores are strong independent prognostic factors of overall CRC patient survival, outperforming tumor TNM criteria and MSI features.

1. STUDY COHORTS AND METHODS

1.1. Study cohorts

The 1st CRC patient cohort (Vilnius cohort) included 101 patients diagnosed with colorectal adenocarcinoma and treated at Vilnius University Hospital Santaros Klinikos (VUH SK, Vilnius, Lithuania) in 2010; the study was approved by and performed in accordance with the guidelines stated by the Lithuanian Bioethics Committee (protocol numbers L-13-03/1 and L-13-03/2). This study was performed with formalin-fixed, paraffin-embedded (FFPE) surgical resection specimens. CD8 IHC slides were prepared as described (see section 1.2.). The clinicopathologic characteristics of the patient cohort are summarized in Table 1.

Table 1. The clinicopathological characteristics (the 1st CRC patient cohort, n = 101)

Clinicopathologic characteristics	Patients, n (%)
Total	101 (100%)
Overall survival (OS), months	
Median	66
Range	2–75
Outcome	
Alive	72 (71.3%)
Deceased	29 (28.7%)
Sex	
Female	60 (59.0%)
Male	41 (41.0%)
Age, years*	
45–70	51 (50.5%)
71–89	50 (49.5%)
Histological grade (G)	
G1	5 (4.9%)
G2	85 (84.2%)
G3	11 (10.9%)
TNM stage	
I	19 (18.8%)
II	38 (37.6%)
III	44 (43.6%)
Tumor invasion (pT)	
pT1	5 (4.9%)

Clinicopathologic characteristics	Patients, n (%)
pT2	19 (18.8%)
pT3	62 (61.4%)
pT4	15 (14.9%)
Lymph node metastasis (pN)	
pN0	57 (56.4%)
pN1	24 (23.8%)
pN2	19 (18.8%)
pN3	1 (1.0%)
Distant metastasis (M)	
M0	101 (100%)

The 2nd CRC patient cohort (Nottingham cohort) included 87 patients diagnosed with colorectal adenocarcinoma (39 with MSI, 48 being microsatellite stable (MSS)) and treated at Nottingham University Hospitals NHS Trust, Queen's Medical Center (NUH QMC, Nottingham, United Kingdom) in 2007–2017; the study was approved by and performed in accordance with the guidelines stated by the Nottingham Health Sciences Biobank (protocol number 15/NW/0685). All FFPE CRC samples were tested by IHC for any expression of DNA mismatch repair proteins, i.e., MLH1, PMS2, MSH2, MSH6 and by PCR, followed by a high-resolution melting analysis for MSI (mononucleotide markers BAT25, BAT26, BCAT25, *MYB* and *EWSR1*), *MLH1* gene promoter methylation, and *BRAF*, *KRAS*, *PIK3CA* gene mutations, as previously described (Susanti S. *et al.*, 2018 and 2019). This study was performed with CD8, CD20, CD68 IHC slides prepared at NUH QMC. The clinicopathologic and molecular characteristics of the patient cohort are summarized in Table 2.

Table 2. The clinicopathologic and molecular characteristics (the 2nd CRC patient cohort (n = 87) grouped by tumor microsatellite instability status)

Clinicopathologic and molecular characteristics	Patients, n (%)		*p* value *
	MSS tumors	**MSI tumors**	
Total	48 (100%)	39 (100%)	
Overall survival (OS), months			
Median	52	46	–
Range	2–97	1–117	
Outcome			
Alive	37 (87.4%)	21 (79.3%)	–
Deceased	11 (12.6%)	18 (20.7%)	
Sex			
Female	23 (47.9%)	26 (66.7%)	0.0878
Male	25 (52.1%)	13 (33.3%)	
Age, years**			
45-71	32 (66.7%)	13 (33.3%)	0.0026*
72-89	16 (33.3%)	26 (66.7%)	
Histological grade (G)			
G2	44 (91.7%)	20 (51.3%)	< 0.0001*
G3	4 (8.3%)	19 (48.7%)	
TNM stage			
I	0	1 (2.6%)	
II	31 (64.5%)	23 (58.9%)	0.9999
III	16 (33.3%)	13 (33.3%)	
IV	1 (2.1%)	2 (5.1%)	
Tumor invasion (pT)			
pT2	1 (2.1%)	1 (2.6%)	
pT3	36 (75.0%)	27 (69.2%)	0.8115
pT4	11 (22.9%)	11 (28.2%)	
Lymph node metastasis (pN)			
pN0	32 (66.6%)	25 (64.1%)	
pN1	8 (16.7%)	8 (20.5%)	0.9027
pN2	8 (16.7%)	6 (15.4%)	
Distant metastasis (M)			
M0	47 (97.9%)	37 (94.9%)	0.5850
M1	1 (2.1%)	2 (5.1%)	
Lymphovascular invasion (LVI)			
LVI0	28 (58.3%)	24 (61.5%)	0.8279
LVI1	20 (41.7%)	15 (38.5%)	
Perineural invasion (Pne)			
Pne0	42 (87.5%)	32 (82.1%)	0.5529
Pne1	6 (12.5%)	7 (18.9%)	
Tumor growth pattern			
Pushing margin	23 (47.9%)	26 (66.7%)	0.0878
Infiltrative margin	25 (52.1%)	13 (33.3%)	

Clinicopathologic and molecular characteristics	Patients, n (%)		_p_ value *
	MSS tumors	MSI tumors	
Total	48 (100%)	39 (100%)	
Tumor budding			
Low (< 10 buds)	33 (68.8%)	25 (64.1%)	0.6557
High (≥ 10 buds)	15 (31.2%)	14 (35.9%)	
Peritumoral lymphocytes			
Inconspicuous	35 (72.9%)	20 (52.6%)	0.0707
Conspicuous	13 (27.1%)	18 (47.4%)	
Primary tumor localization			
Left colon	28 (58.3%)	3 (7.7%)	< 0.0001*
Transverse colon	0	1 (2.6%)	
Right colon	19 (39.6%)	33 (84.6%)	
Multiple sites	1 (2.1%)	2 (5.1%)	
BRAF gene[†]			
Wild type	44 (91.7%)	18 (46.2%)	< 0.0001*
Mutant	4 (8.3%)	21 (53.8%)	
KRAS gene[†]			
Wild type	25 (52.1%)	32 (82.2%)	0.0060*
Mutant	23 (47.9%)	7 (17.9%)	
PIK3CA gene[†]			
Wild type	40 (83.3%)	31 (79.5%)	0.7822
Mutant	8 (16.7%)	8(20.5%)	

* Fisher's exact test with significance level α = 0.05. [†] _BRAF_ gene was tested for point mutations in exons 11 and 15, _KRAS_ gene was tested for point mutations in exons 2, 3 and 4, _PIK3CA_ gene was tested for point mutations in exons 1, 9 and 20
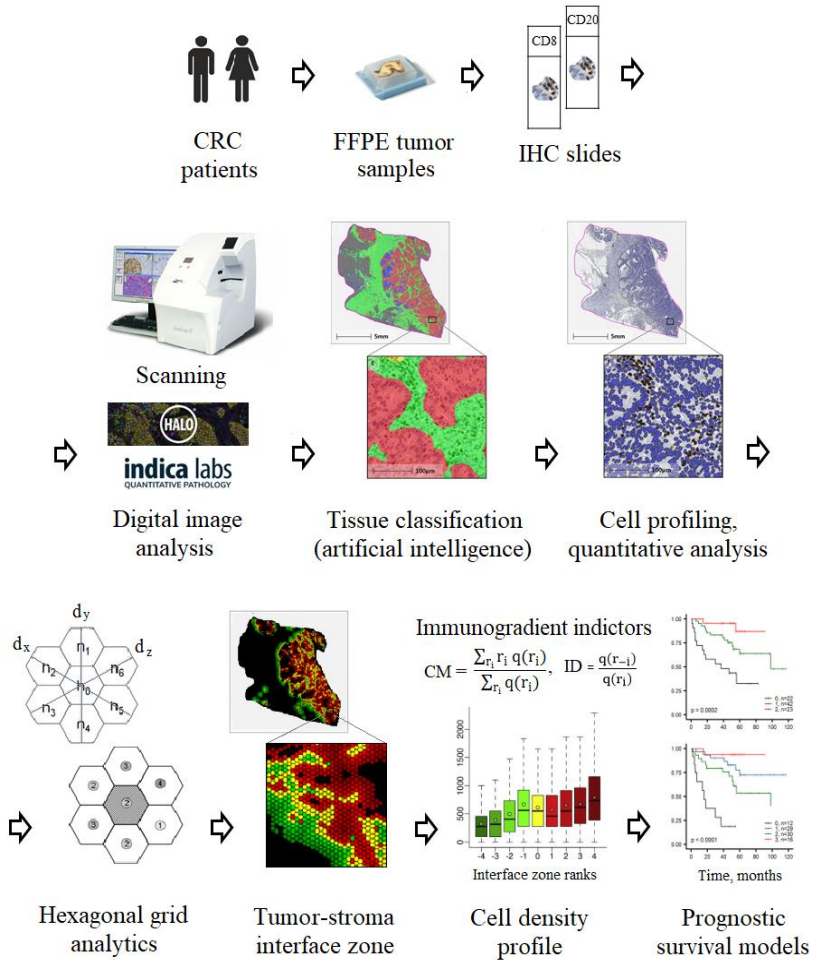
1.2. Immunohistochemical staining

The FFPE tumor tissue sections were cut at 3 μm thickness and mounted on positively charged slides. IHC staining was performed using the Roche Ventana BenchMark ULTRA (_Ventana Medical Systems_, USA) automated slide stainer. Monoclonal antibodies against cytotoxic T-cell marker CD8 (clone C8/144 B; dilution 1:400; _Cell Marque_, USA) were used, followed by use of an ultraView Universal DAB Detection kit (_Ventana Medical Systems_, USA). Tissue sections were counterstained with Mayer hematoxylin. Positive staining controls were performed using FFPE human tonsil tissue.

1.3. Digital pathology workflow

The stages of the digital pathology workflow in this study are presented in Figure 1: first, CRC sample FFPE tumor sections are IHC stained for immune markers and digitized by scanning; the WSI are then transferred to a DIA platform; the artificial intelligence-based tissue classifier is trained to segment tissue into tumor epithelium, stroma, and other classes; a quantitative analysis of tissue cell populations in the TME is performed using a cell profiling module; DIA data are analysed by applying spatial hexagonal grid-based analytics: the tumor-stroma interface zone (IZ) and cell distribution (density) profiles in the IZ are extracted; the spatial aspects of cell distribution in the IZ are then expressed based on Imunogradient indicators, e.g., Center of Mass (CM) and Immunodrop (ID) for the mean cell density; finally, the prognostic value of immune response indicators is evaluated within the context of clinicopathological indicators, and combined prognostic models to predict patient survival are developed.

CRC patients

FFPE tumor samples

IHC slides

CD8   CD20

Scanning

indica labs
QUANTITATIVE PATHOLOGY

Digital image analysis

Tissue classification (artificial intelligence)

Cell profiling, quantitative analysis

d_y d_x d_z
n_1 n_2 n_6 n_0 n_3 n_5 n_4

Hexagonal grid analytics

Tumor-stroma interface zone

Immunogradient indictors

$$CM = \frac{\sum_{r_i} r_i\, q(r_i)}{\sum_{r_i} q(r_i)}, \quad ID = \frac{q(r_{-i})}{q(r_i)}$$

Interface zone ranks

Cell density profile

Time, months

Prognostic survival models

Figure 1. Digital pathology workflow

1.3.1. Digitization of histology slides

CD8 IHC slides (prepared at VUH SK) and CD8, CD20, CD68 IHC slides (prepared at NUH QMC) were scanned using a *ScanScope XT Slide Scanner* (*Leica Aperio Technologies*, CA, USA) or an *Aperio*

AT2 Slide Scanner (*Leica Microsystems*, Wetzlar, Germany) with 20x magnification (0.5 μm resolution). Digitized WSIs were archived in a pathology image database *ImageScope* (version 11.1.2.752, *Leica Biosystems*, Chicago, USA), then transferred to a DIA platform HALO™ (version 2.2.1870, *Indica Labs*, New Mexico, USA).

1.3.2. Tumor tissue classification

The artificial intelligence-based supervised HALO AI classifier was used for tissue segmentation. Overall 4 CRC tissue classifiers were developed for CD8 IHC slides (prepared at VUH SK) and CD8, CD20, CD68 IHC slides (prepared at NUH QMC). Tissue classifiers were trained to segment CRC tissue into tumor epithelium (tumor), stroma, necrosis, lymphoid aggregates, and background (consisting of glass, mucus areas, artefacts).

1.3.3. Cell population quantitative analysis

The HALO Multiplex IHC module (version 1.2) was used for a quantitative analysis of different cell populations in TME. Four cell profiling algorithms were developed for CD8 IHC slides (prepared at VUH SK) and CD8, CD20, CD68 IHC slides (prepared at NUH QMC). The algorithms were calibrated to detect cells with hematoxylin-stained nuclei and cells with cytoplasmic expression of IHC markers.

1.3.4. Tumor-stroma interface zone detection

We have developed a digital pathology methodology for the automated detection of the tumor-stroma IZ and profiling of immune cell distribution in the IZ using novel Immunogradient indicators (International Patent Application No. PCT/IB2020/053396, World Intellectual Property Organization International Bureau). The method

is based on DIA data subsampling and quantitative spatial analysis in WSI by a hexagonal grid. IZ detection and the computation of hexagonal data variables were implemented in C++ (g++ 7.3.8) using *libtiff* version 5.2.4. (https://www.libtiff.org) and *Boost* version 1.67 (https://www.boost.org). The method is described in details by Rasmusson *et al.*, 2020.

The IZ is detected by processing data obtained by the tissue classifier (tissue class for each pixel in WSI). In brief, the tumor edge (TE) is computed based on changes in tissue class area fractions inside each hexagon. TE consists of hexagons on the interface between the tumor and stroma; the remaining hexagons are classified as tumor, stroma or background. The distance from each tumor and stroma hexagon to the nearest TE is then calculated, hexagons are ranked so that hexagons at the TE have rank 0 (distance 0), tumor hexagons are assigned a rank equal to their distance from the nearest TE (the tumor aspect (T) rank in the IZ), and stroma hexagons are assigned a rank equal to their negative distance to the nearest TE (the stroma aspect (S) rank in the IZ). This allows extracting the IZ of any width, e.g., an IZ of width 9 covers ranks [–4; 4] (Figure 2).
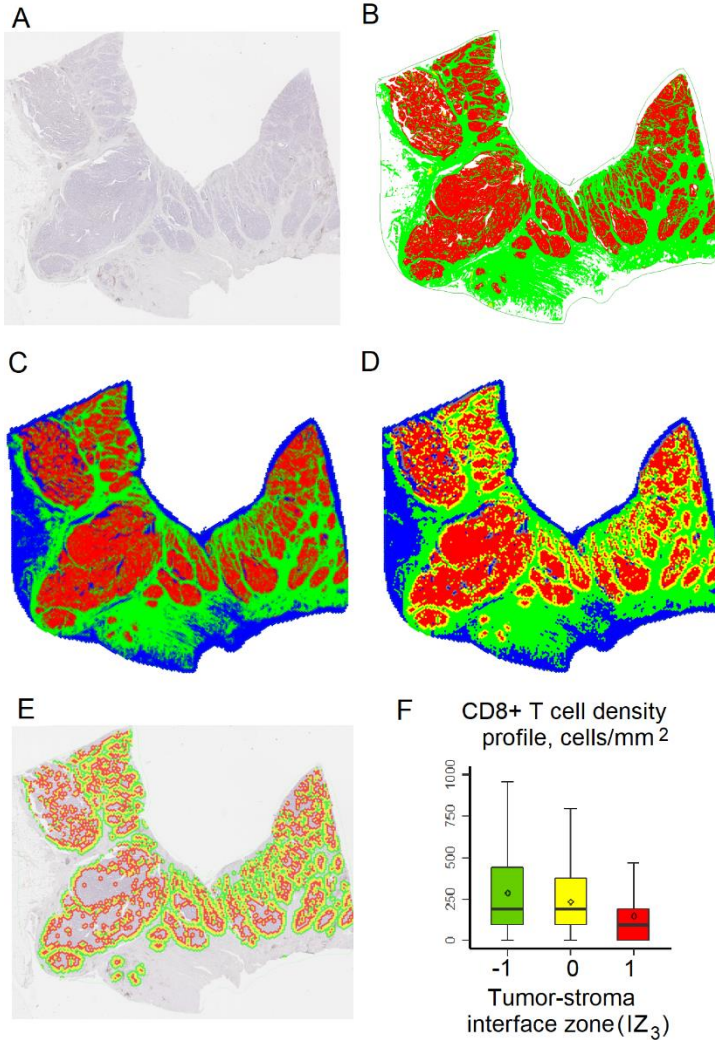
Figure 2. Tumor edge (TE), tumor-stroma interface zone (IZ) and CD8+ T cell density profile extraction: (A) DIA input: WSI of CRC tumor section IHC stained for CD8; (B) the same WSI analysed by the tissue classifier: tumor parts are red, stroma parts green, and background white; (C) the tissue class areas in the same WSI are subsampled by hexagonal grid: tumor parts are red, stroma parts green, and background blue; hexagon side length is 65 μm; (D) extracted TE (yellow; rank = 0); (E) stroma (green; rank = −1), and tumor (red; rank =1) aspects of 3 rank wide interface (IZ_3); (F) CD8+ cell density profile within IZ_3, colours and ranks correspond to (E).

1.3.5. Immune response indicators

The data of immune cell profiling (cell coordinates) are subsampled by the same hexagonal grid used for the subsampling of tissue classifier data so that cell counts and densities can be calculated in each hexagon and summarized in the ranks. The rank data are further used to compute immune response indicators, i.e., mean cell densities (and standard deviations) in the TE, tumor or stroma aspects of the IZ. Subsequently, the ranking allows plotting cell density profiles across the IZ (Figure 2, F; the IZ width of 3 ranks was found optimal for CRC (see section 2.1.)) and computing Immunogradient indicators that reflect cell density change (gradient) in the stroma-to-tumor direction. Immunogradient indicators were found to be the strongest in predicting the OS of patients in this study:

- **Center of Mass (CM)** estimates the cell density gradient towards the tumor aspect of the IZ – it shows the propensity of cells to infiltrate the tumor epithelium:

$$CM(q) \; = \; \frac{\sum_{r_i} r_i \, q(r_i)}{\sum_{r_i} q(r_i)},$$

where r_i - IZ ranks when $r_i \in [-i; i]$, $q(r_i)$ is a variable, e.g., the mean CD8 + T cell density, calculated in the corresponding IZ rank.

- **Immunodrop (ID)** estimates a change (decrease) in cell density across the TE:

$$ID = \frac{q(r_{-i})}{q(r_i)},$$

where r_i - IZ ranks when $r_i \in [-i; i]$, $q(r_{-i})$ and $q(r_i)$ are variables, e.g., the mean CD8 + T cell density, calculated in the stroma and tumor aspect ranks of the IZ, respectively.

1.4. Statistical analysis

Immune response indicators are based on means and standard deviations of immune cell densities (cell counts/tumor and stroma tissue area, mm^2). The distributions of indicator values revealed a right asymmetry (based on the Kolmogorov-Smirnov test); therefore, logarithm-transformed values were used for parametric statistics. The strongest indicators were found using Cox regression and leave-one-out cross-validation tests (Rushing C. *et al.*, 2015). The statistical significance of cell density variations in the IZ and tumor compartment, also among tumors of different pathologic characteristics, were tested using one-way ANOVA, followed by Bonferroni's post-hoc test for pairwise comparisons and a two-sided Welch's t-test for the homogeneity of variances. Fisher's exact and χ2 tests were applied to evaluate the independence of qualitative characteristics. A Pearson correlation matrix was used to evaluate the relationships between immune response indicators. A factor analysis of immune indicators was performed using the factoring method of principle component analysis and general orthomax rotation; factors were retained with eigenvalues ≥ 1. Overall survival (OS) was calculated as the time from the surgery to death due to any cause. The OS distributions for the patients were estimated using the Kaplan-Meier function; a log-rank test was used to evaluate the difference between survival curves. The *Cutoff Finder* tool (version 2.1; Charité University, Berlin, Germany) (Budczies J. *et al.,* 2012) was used to determine a cutoff value for each indicator to test univariate and multivariate predictions of OS. Risk factors for OS were assessed by Cox regression models obtained by a stepwise likelihood ratio test; models were generated to include statistically significant indicators identified by univariate analysis and with no linear correlations (r < 0.9). A leave-one-out cross-validation test was used to validate the Cox models. A two-tailed *p* value less than 0.05 was considered to be significant. Statistical analysis was performed using the SAS software package (version 9.4; SAS Institute Inc., Cary, NC, USA).

2. RESULTS

2.1. Tumor edge and tumor-stroma interface zone
### (1st CRC patient cohort)

DIA data of CRC sample WSIs (tissue class areas, CD8+ T cell coordinates) were sampled and analysed by the hexagonal grid analytics. The tumor-stroma IZ detection algorithm classified grid elements into the tumor edge (TE), tumor, stroma classes (Figure 2, E). A visual evaluation of WSIs showed that TE was not representative in 4 tumors (excluded from further analysis): 3 tumors were of the mucinous subtype (extracellular mucin accounts $> 50\%$ of the tumor volume), therefore, the fragments of tumor epithelium surrounded by mucus do not have contact with the solid part of the tumor and are not involved in the extraction of TE (Figure 3, A1-3); 1 tumor had an infiltrative growth pattern, with the total tumor epithelium area being 4.2 mm^2 (Figure 3, B1-3), and thus the minimum tumor epithelium area required for the TE extraction was considered to be at least 4.5 mm^2.
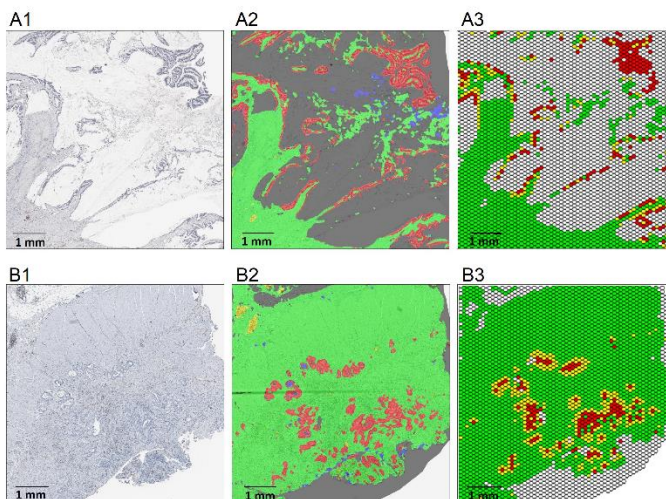
Figure 3. Examples of cases with not representative tumor edge: A – mucinous CRC subtype, B – CRC of infiltrative growth pattern (total tumor epithelium area 4.2 mm^2), where: A1 and B1 – WSI fragments IHC stained for CD8, A2 and B2 – same fragments analysed by the tissue classifier: tumor (red), stroma (green), necrotic tissue

(blue), background (black; includes glass and mucus areas) classes; A3 and B3 – same fragments analysed by the IZ detection algorithm: grid elements correspond to TE (yellow), tumor (red), stroma (green), background (grey) classes.

The tumor-stroma IZ of 3, 5, 7 or 9 rank width, and TE of 1 or 3 rank width, i.e., IZ_3 (ranks [–1; 1]), IZ_5 (ranks [–2; 2]), IZ_7 (ranks [–3; 3]) or IZ_9 (ranks [–4; 4]), and TE_1 (rank 0) or TE_3, (ranks [–1; 1]), respectively, were used in this study. A total of 7 different IZ variants were extracted (Figure 4).
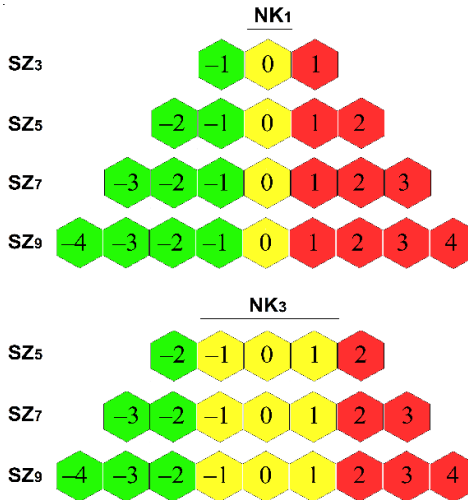
Figure 4. Different variants of tumor-stroma interface zone: IZ_3, IZ_5, IZ_7 and IZ_9 correspond to IZ of 3, 5, 7 and 9 rank width; TE_1 and TE_3 correspond to TE of 1 and 3 rank width. The colours reflect stroma (green), TE (yellow) and tumor (red) aspects of the IZ.

The mean number and standard deviation of hexagonal grid elements in the ranks of IZ_9 decreased with the distance from TE ($p < 0.05$; data not shown). Most of the grid elements were in the rank interval $r_i \in [–1; 1]$. The mean number and standard deviation of grid elements in the ranks –1 and 1 was similar ($p > 0.05$) (Figure 5).
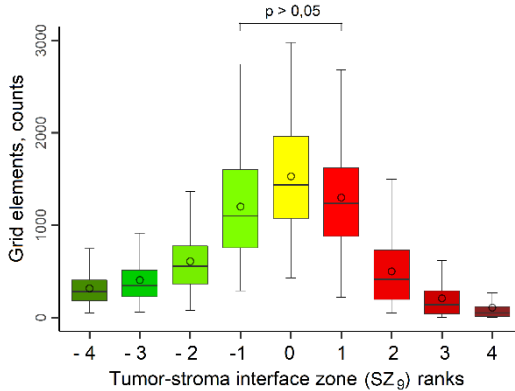
Figure 5. The number of grid elements in the ranks of the tumor-stroma interface zone (IZ_9) (1st CRC patient cohort, n = 101). The colours reflect stroma (green), TE (yellow) and tumor (red) aspects of the IZ

The CD8+ T cell mean densities and standard deviations were higher in the stroma aspect of the IZ_9 ($p < 0.05$; data not shown). There were no differences in the CD8+ T cell mean densities and standard deviations between the ranks of the stroma aspect, as well as between the ranks of the tumor aspect of the IZ_9; however, the change in cell density between the TE (rank 0) and the neighbouring stroma (rank –1) or tumor (rank 1) ranks was observed (Figure 6).
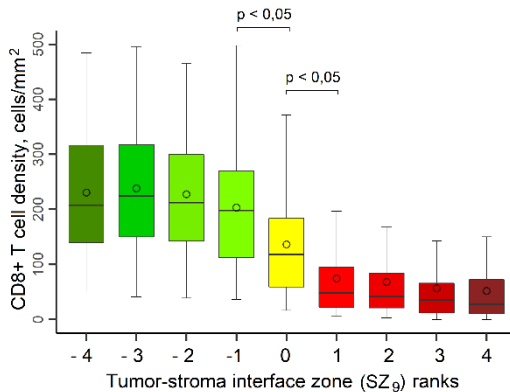
Figure 6. CD8+ T cell density in the ranks of the tumor-stroma interface zone (IZ_9) (1st CRC patient cohort, n = 101). The colours reflect stroma (green), TE (yellow) and tumor (red) aspects of the IZ

In all IZ variants CD8+ T cell density indicators were calculated: CD8+ T cell density means and standard deviations in the stroma, TE and tumor aspects of the IZ, and Immunogradient indicators, i.e., Center of Mass (CM) and Immunodrop (ID) for CD8+ T cell density mean and standard deviation. The strongest prognostic indicators were selected by multivariate Cox regression followed by a leave-one-out cross-validation: among all absolute CD8+ T cell density indicators in the IZ, the strongest was the mean CD8+ T cell density in the tumor aspect of the IZ_3 (rank 1) (65 counts); among CM indicators computed in all IZs, the strongest was the CM for the mean CD8+ T cell density in the IZ_3 (65 counts); the model with ID for the mean CD8+ T cell density between ranks –1 and 1 and ID for the CD8+ T cell density standard deviation between ranks 0 and 1 was extracted 96 times (Table 3).

Table 3. Cox regression models by leave-one-out cross-validation (the 1st CRC patient cohort, n = 101)

Model indicators (absolute cell density indicators)	Model counts	χ^2	*p* value	HR	95% CI
IZ_3, when TE_1: CD8_d_T	65	9.26	0.0024	0.35	0.18-0.69
IZ_5, when TE_1: CD8_d_T	21	9.11	0.0028	0.35	0.17-0.69
IZ_7, when TE_3: CD8_sd_T	15	9.73	0.0019	0.32	0.16-0.66
Model indicators (CM indicators)	**Model counts**	χ^2	***p* value**	**HR**	**95% CI**
IZ_3: CD8_CM_d	65	10.22	0.0014	0.33	0.16-0.65
IZ_7: CD8_CM_d	36	10.24	0.0015	0.32	0.16-0.64
Model indicators (ID indicators)	**Model counts**	χ^2	***p* value**	**HR**	**95% CI**
CD8_ID_d, when r_{-1}/r_1 CD8_ID_sd, when r_0/r_1	96	4.48	0.0347	3.29	1.09-9.92
CD8_ID_d, when r_{-1}/r_0 CD8_ID_sd, when r_0/r_1	5	4.78	0.0031	2.18	1.08-4.40

SZ_3, SZ_5, SZ_7 – tumor-stroma interface zone of 3, 5 or 7 rank width, respectively; TE_1, TE_3 – TE of 1 or 3 rank width, respectively; CD8_d – mean CD8+ T cell density; CD8_sd – CD8+ T cell density standard deviation; T – the tumor aspect of the IZ; CM_d – Center of Mass for the mean cell density; ID_d – Immunodrop for the mean cell density between ranks -1 and 1 (r_{-1}/r_1) or between ranks -1 and 0 (r_{-1}/r_0); ID_sd – Immunodrop for the cell density standard deviation between ranks 0 and 1 (r_0/r_1).

In summary, the results revealed that most of the grid elements were in the rank interval $r_i \in [-1; 1]$, significant CD8+ T cell density differences between neighbouring ranks were found only in the rank range $r_i \in [-1; 1]$, and the strongest prognostic indicators of CD8+ T cell response in CRC samples were obtained by a 3 rank wide IZ. To conclude, IZ_3 (further called IZ) was the most informative and thus used for further analysis of immune response in the TME.

2.2. Immune response in colorectal cancer microenvironment (1st CRC patient cohort)

2.2.1. Summary statistics of immune response indicators

The distribution of cytotoxic T cells (CD8+) in the TME was assessed by immune response indicators (Table 4):

   – absolute cell density means and standard deviations in the stroma (rank –1), TE (rank 0) and tumor (rank 1) aspects of the IZ;

   – absolute cell density mean and standard deviation in the whole tumor, i.e., in all grid elements assigned to the tumor class (intratumoral cell density);

   – Immunogradient indicators: CM which reflects cell density gradient towards the tumor aspect in the IZ, and ID which reflects cell density change (decrease) across the TE.

Table 4. Summary statistics of immune response indicators (1st CRC patient cohort, n = 101)

Immune response indicators	Mean	Mdn	SD
CD8_d_S	251.45	210.81	216.44
CD8_sd_S	313.07	283.19	174.77
CD8_d_TE	177.94	121.05	194.68
CD8_sd_TE	245.00	213.62	166.56
CD8_d_T	93.88	49.11	137.10
CD8_sd_T	122.91	106.47	91.00
CD8_d_INT	90.62	49.64	138.11
CD8_sd_INT	119.51	98.65	92.01
CD8_CM_d	-0.38	-0.37	0.15
CD8_CM_sd	-0.30	-0.29	0.12

Immune response indicators	Mean	Mdn	SD
CD8_ID_d	4.93	3.61	3.69
CD8_ID_sd	3.12	2.67	1.53
CD8_ID*_d	2.70	2.39	1.33
CD8_ID*_sd	2.21	2.04	0.86

CD8_d – mean CD8+ T cell density (cells/mm^2); CD8_sd – CD8+ T cell density standard deviation; TE – tumor edge of the IZ; S – stroma aspect of the IZ; T – tumor aspect of the IZ; INT – intratumoral; CM_d or CM_sd – Center of Mass for mean cell density or standard deviation, respectively; ID_d or ID_sd – Immunodrop for mean cell density or standard deviation between ranks -1 and 1, respectively; ID_d* or ID_sd* – Immunodrop for mean cell density or standard deviation between ranks 0 and 1, respectively.

CD8+ T cell density was highest and most dispersed in the stroma aspect, less abundant and dispersed in the TE, and lowest and less dispersed in the tumor aspect of the IZ (p < 0.05; data not shown); CD8+ T cell density in the tumor aspect of the IZ and intratumoral CD8+ T cell density did not differ (p > 0.05; data not shown).

2.2.2. Associations between immune response indicators and pathological features

The association analysis (data not shown) revealed that CD8+ T cell densities in the stroma, TE and tumor aspects of the IZ, intratumoral CD8+ T cell density were higher in pT1-2 and pN0 tumors (p < 0,05), and the CD8+ T cell density gradient towards the tumor aspect of the IZ was higher (by higher CM and lower ID values) in pT1-2 tumors (p < 0,05). Thus, CD8 + T cells were more abundant and infiltrative in early stage tumors. However, no statistically significant associations between immune response indicators and histological tumor grade, patient age, and sex were found.

2.2.3. Correlations of immune response indicators

Linear positive correlations were found between means and standard deviations of CD8+ T cell density in different aspects of the IZ and the whole tumor (r > 0.9, p < 0.0001), also between the mean CD8+

T cell density in the stroma/tumor aspect and TE of the IZ, as well as between the tumor aspect of the IZ and in the whole tumor ($r > 0.9$, $p < 0.0001$); ID indicators for the mean cell density and standard deviation between ranks –1 and 0 or –1 and 1 were strongly correlated with each other, too ($r > 0.9$, $p < 0.0001$); also, a strong negative correlation between CM and ID indicators was found ($r > –0.9$, $p < 0.0001$). Based on these results, Cox regression models were developed using indicators with no linear correlations ($r < 0.9$), while CM and ID indicators were analysed separately.

2.2.4. The prognostic value of immune response indicators

The statistics of univariate analyses by clinical, pathological and immune response indicators are presented in the Table 5. Patient age, primary tumor invasion stage, lymphnode metastases status, TNM stage, and all selected immune response indicators were significantly associated with patient OS ($p < 0.05$). Immune response indicator values were stratified into high and low values according to cut-off values (Table 5).

Table 5. Statistics of univariate analyses of clinical, pathological and immune response indicators for patient overall survival (1st CRC patient cohort, $n = 101$). cf – cut-off values detected by log-rank test (Cutoff Finder (Budczies J. *et al.*, 2012)) *$p < 0,05$

| Indicators	Category	*p* value	HR	95% CI
Sex	male	0.1974	1.56	0.79–3.05
Age	> 70 years	0.0441*	2.06	1.02–4.17
G	G3 (*versus* G1-2)	0.3379	1.59	0.62–4.12
pT	pT3-4 (*versus* pT1-2)	0.0106*	6.47	1.55–27.1
pN	pN1-3 (*versus* pN0)	0.0214*	2.23	1.13–4.42
TNM stage	III (*versus* I-II)	0.0214*	2.23	1.13–4.42
CD8_d_S	high, when cf = 5.85	0.0080*	0.11	0.02–0.80
CD8_d_T	high, when cf = 3.36	0.0014*	0.35	0.18–0.69
CD8_d_INT	high, when cf = 4.23	0.0011*	0.23	0.09-0.61
CD8_CM_d	high, when cf = -0.52	0.0008*	0.33	0.17–0.65
CD8_CM_sd	high, when cf = -0.31	0.0054*	0.39	0.19–0.77
CD8_ID_d	high, when cf = 2.03	0.0005*	3.20	1.60–6.41
CD8_ID*_sd	high, when cf = 1.04	0.0028*	2.69	1.37–5.28

Cox regression models (LR: 22.55 and 21.56, p < 0.0001) revealed 4 independent prognostic factors (Table 6): patient age of over 70 years (p ≤ 0.0453) and advanced primary tumor invasion stage (p ≤ 0,0177) were associated with shorter patient OS; high CM for the CD8+ T cell density was a strong factor for longer patient OS (p = 0.0071, Model 1); in contrast, high ID for the CD8+ T cell density was a strong factor for shorter patient OS (p = 0.0126, Model 2). Thus, these models reveal that Immunogradient indicators (CM and ID) for the CD8+ T cell density are stronger patient OS predictors than the absolute CD8 + T cell density in the IZ and the intratumoral CD8+ T cell density indicators. Compared to ID for the CD8+ T cell density (χ^2 = 6.22, Model 2), CM for the CD8+ T cell density (further called – CD8 Immunogradient; χ^2 = 7.25, Model 1) was a statistically stronger prognostic factor.

Table 6. Multivariate Cox regression models for patient OS (1st CRC patient cohort, n = 101)

Model 1 LR: 22.54, p < 0.0001	χ^2	*p* value	HR	95% CI
Age (> 70 years)	4.01	0.0453	2.04	1.02–4.09
pT stage (pT 3-4)	6.19	0.0128	6.22	1.48–26.21
CD8_CM_d (high)	7.25	0.0071	0.39	0.20–0.77
Model 2 LR: 21.56, p < 0.0001	χ^2	*p* value	HR	95% CI
Age (> 70 years)	4.13	0.0432	2.06	1.03–4.13
pT stage (pT 3-4)	5.62	0.0177	5.78	1.36–24.63
CD8_ID_d (high)	6.22	0.0126	2.44	1.21–4.92

Kaplan-Meier survival curves obtained by the independent factors are presented in Figure 7: the probability of 5-year OS was 80% in patients under 70 years and 63% in elderly patients; the 5-year OS rate was 92% in case of the early primary tumor invasion stage (pT1-2) and 65% in case of the advanced primary tumor invasion stage (pT3-4). The CD8 Immunogradient stratified patients into prognostic groups with 77% and 52%; similarly, ID for the CD8 + T cell density

stratified patients into groups with 76% and 50% 5-year OS probabilities.
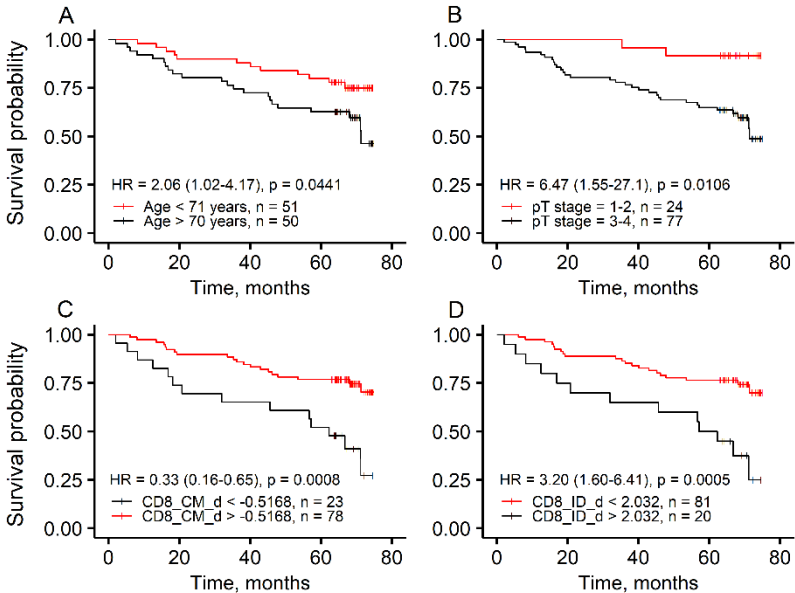
Figure 7. Kaplan-Meier survival curves obtained by independent clinicopathological and Immunogradient indicators for patient overall survival: A – patient age; B – primary tumor invasion stage (pT); C – CD8 Immunogradient (CD8_CM_d); D – ID for CD8+ T cell density (CD8_ID_d).

2.2.4. Factor analysis of immune response indicators

A factor analysis of immune response indicators identified 2 independent factors (Figure 8): Factor 1 was described by CD8+ T cell density means and standard deviations in all the aspects of the IZ, reflecting the absolute CD8+ T cell density in the IZ (Figure 8, B); Factor 2 was described by CM and ID for CD8+ T cell density and standard deviation (Immunogradient indicators), which reflects the CD8+ T cell density gradient across the IZ (Figure 8, C), i.e., the change of cell density in the direction of stroma-to-tumor in the IZ: higher values correspond to a higher propensity of CD8+ T cells

31

towards the tumor aspect in the IZ. These results show that the quantitative and spatial (gradient) characteristics of the CD8+ T cell distribution in the IZ are linearly independent. To integrate the predictive power of both factors, their values were combined by calculating an aggregated CD8+ T cell response in the IZ factor. The values of the immune response factors were stratified into high and low value categories according to the cut-off values (data not shown).
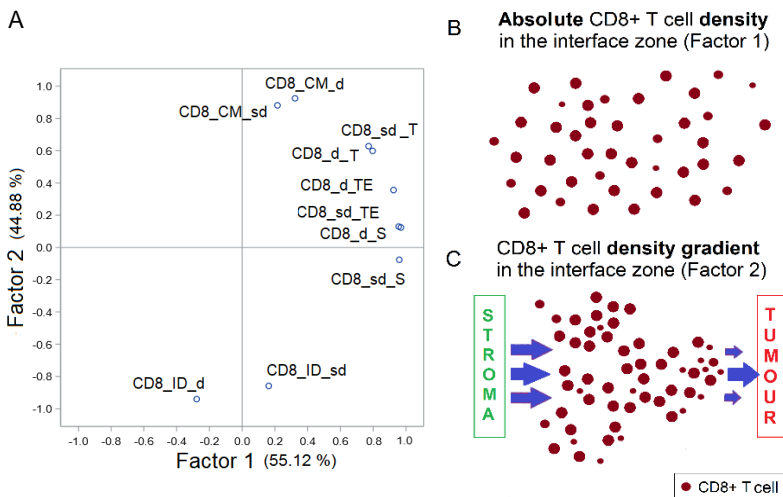
Figure 8: Factor analysis of immune response indicators: A: Factor 1, absolute CD8+ T cell density in the IZ (B) factor, that includes indicators of CD8+ T cell densities and standard deviations in the stroma, TE, and tumor aspects of the IZ; Factor 2, CD8+ T cell density gradient across the IZ (C) factor, that includes Immunogradient indicators for CD8+ T cell density and standard deviation and reflects the propensity of cells to infiltrate towards the tumor. Brown colour circles represent CD8+ T cells.

Cox regression models (LR: 21.8, p < 0,0001) revealed 4 independent prognostic factors (Table 7): patient age of over 70 years (p ≤ 0,0375) and an advanced primary tumor invasion stage (p ≤ 0,0260) were associated with shorter patient OS; high score of the CD8+ T cell density gradient across the IZ factor (p = 0.0112, Model 3), and a high score of the aggregated CD8+ cell response in the IZ factor (p = 0.0196, Model 4), were associated with longer patient OS.

Table 7. Multivariate Cox regression models for patient overall survival (the 1st CRC patient cohort, n = 101)

Model 3 LR: 21.82, p <0.0001	χ^2	*p* value	HR	95% CI
Age (>70 years)	4.33	0.0375	2.09	1.04-4.20
pT stage (pT 3-4)	6.23	0.0126	6.25	1.48-26.38
Factor 2:CD8+ T cell density gradient across the IZ (high)	6.43	0.0112	0.41	0.21-0.82
Model 4 LR: 21.85, p <0.0001	χ^2	*p* value	HR	95% CI
Age (>70 years)	5.13	0.0235	2.24	1.12-4.50
pT stage (pT 3-4)	4.96	0.0260	5.25	1.22-22.61
Aggregated factor: CD8+ T cell response in the IZ (high)	5.45	0.0196	0.41	0.19-0.87

Kaplan-Meier survival curves by independent factors are presented in Figure 9: Factor 2 stratified patients into groups with 77% and 54% 5-year OS probabilities. Aggregated factor dichotomized patients into groups with 84% and 58% 5-year OS probabilities.
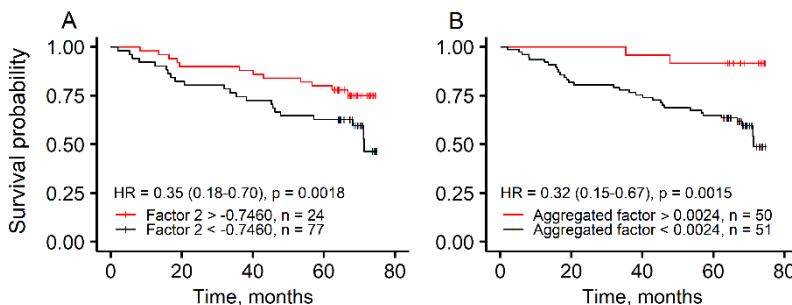
Figure 9. Kaplan-Meier survival curves obtained by independent factors for patient overall survival: A – Factor 2: CD8+ T cell gradient across the IZ; B – Aggregated factor: CD8+ T cell response in the IZ.

These results confirm that the CD8+ T cell density gradient across the IZ is a statistically stronger prognostic factor than the absolute CD8 + T cell density in the IZ.

2.3. Immune response in colorectal cancer microenvironment
(2nd CRC patient cohort)

2.3.1. Summary statistics of immune response indicators

The distributions of cytotoxic T cells (CD8+), B cells (CD20+) and macrophages (CD68+) in the TME were assessed by immune response indicators (Table 8):

– absolute cell density means in the stroma (rank –1), TE (rank 0) and tumor (rank 1) aspects of the IZ;

– absolute cell density mean in the whole tumor, i.e., in all grid elements assigned to the tumor class (intratumoral cell density);

– Immunogradient indicators: CM reflecting the cell density gradient towards the tumor aspect in the IZ.

Table 8. Summary statistics of immune response indicators (the 2nd CRC patient cohort, n = 87) grouped by tumor microsatellite instability status)

Immune response indicators	MSS tumors, n = 48			MSI tumors, n = 39			p value*
	Mean	Mdn	SD	Mean	Mdn	SD	
CD8_d_S	193.8	147.1	147.7	370.8	294.9	404.6	0.0024*
CD8_d_TE	141.8	90.0	128.4	339.9	208.2	400.5	0.0004*
CD8_d_T	76.5	49.2	92.4	262.4	140.2	342.6	0.0001*
CD8_d_INT	65.4	37.5	81.9	238.9	133.4	311.2	<0.0001*
CD8_CM_d	-0.35	-0.35	0.17	-0.20	-0.18	0.21	0.0006*
CD20_d_S	54.3	32.8	68.4	71.3	36.7	83.3	0.3650
CD20_d_TE	31.6	14.0	59.3	30.5	18.9	33.4	0.7857
CD20_d_T	12.2	4.6	30.6	5.4	3.8	6.1	0.0899
CD20_d_INT	13.8	4.1	31.2	9.7	5.8	12.9	0.6003
CD20_CM_d	-0.49	-0.54	0.23	-0.59	-0.63	0.14	0.0141*
CD68_d_S	173.9	158.1	118.2	182.4	173.8	104.3	0.5616
CD68_d_TE	145.1	120.2	99.7	190.1	175.1	106.0	0.0281*
CD68_d_T	72.4	55.2	73.4	126.5	100.3	82.4	<0.0001*
CD68_d_INT	60.1	48.9	55.8	112.1	95.3	71.4	<0.0001*
CD68_CM_d	-0.20	-0.28	0.14	-0.11	-0.08	0.14	<0.0001*

CD8_d – mean CD8+ T cell density (cells/mm^2); CD20_d – mean CD20+ B cell density (cells/mm^2); CD68_d – mean CD68+ macrophage density (cells/mm^2); TE – tumor edge of the IZ; S – stroma aspect of the IZ; T – tumor aspect of the IZ; INT – intratumoral; CM_d – Center of ass for mean cell density

CD8+ T cell and CD68+ macrophage densities in the IZ and the whole tumor and density gradients towards the tumor (CM indicators) were higher in MSI tumors ($p < 0.05$), whereas CD20+ B cell densities in the IZ and the whole tumor were similar in MSI and MSS tumors; however, the CD20+ B cell density gradient towards the tumor aspect of the IZ was lower in MSI tumors ($p < 0.05$) (Table 8) – this is explained by a higher B cell infiltrate in the tumor periphery observed in MSI tumors.

CD8+ T cell densities both in the IZ and the whole tumor were higher than CD68+ macrophage densities in the same regions in MSI tumors ($p < 0.05$; data not shown), however, the densities of these cells did not differ in MSS tumors; CD20+ B cell densities were lowest both in MSI and MSS tumors ($p < 0.05$; data not shown).

CD8+ T cells, CD20+ B cells and CD68+ macrophages were least abundant in the tumor aspect and more abundant in the TE aspect of the IZ both in MSI and MSS tumors ($p < 0.05$; data not shown); CD8+ T cell and CD68+ macrophage densities were similar in the stroma and TE aspects, whereas CD20+ B cell density was higher in the stroma aspect compared to the TE aspect of the IZ ($p < 0.05$; data not shown). No statistically significant differences were found between CD8+, CD20+, and CD68+ cell densities in the tumor aspect of the IZ and in the whole tumor (data not shown).

2.3.2. Associations between immune response indicators and pathological features

The association analysis (data not shown) revealed that in MSI tumors, lower immune cell densities in the IZ and the whole tumor, as well as a lower immune cell density gradient towards the tumor were associated with tumor progression, i.e., with tumors of pT4 or pN1-2 stage, also with perineural invasion, lymphovascular invasion, and high tumor budding ($p < 0,05$). In MSS tumors, immune cells were more abundant/infiltrative in tumors of poor differentiation by histology or with the pushing tumor margin ($p < 0,05$). However,

unlike in MSI tumors, in MSS tumors, the CD68+ macrophage density gradient towards the tumor was higher in cases with advanced tumor invasion (pT4) and lymph node metastasis (pN1-2) (p < 0,05) – this may be explained by difference in M1 type (pro-inflammatory) macrophage percentage in MSI and MSS tumors (Narayanan S. *et al.*, 2019). No statistically significant associations between immune response indicators and patient sex, age, tumor location, and molecular markers were detected.

2.3.3. Correlations of immune response indicators

The correlation matrix of immune response indicators showed: a linear positive correlation between CD8+ T cell densities in the stroma and TE aspects of the IZ, also between the tumor and TE aspects of the IZ, or in the whole tumor (r > 0.9, p < 0.0001); linear positive correlations were found of CD68+ macrophage densities between the stroma and TE aspects of the IZ, and between the tumor and TE aspects of the IZ (r > 0.9, p < 0.0001). The CD8+ T cell with CD20+ B cell or CD68+ macrophage density indicators, as well as the CD20+ B cell with CD68+ macrophage density indicators had moderate/weak (r < 0.6, p < 0.05) or no correlation.

2.3.4. The prognostic value of immune response indicators

The statistics of univariate analyses by clinical, pathological and immune response indicators are presented in Table 9. Tumor growth pattern (by visual assessment), CM for CD8+ T and CD20+ B cell densities, CD20+ B cell density in the stroma and tumor aspects of the IZ and in the whole tumor were significantly associated with patient OS (p < 0.05). The association between CD68+ macrophage response indicators and patient OS was not statistically significant and therefore was not analysed further. Immune response indicator values were

stratified into high and low values according to cut-off values (Table 9).

Table 9. Statistics of univariate analyses of clinical, pathological and immune response indicators for patient overall survival (the 2nd CRC patient cohort, n = 87). cf – cut-off value detected by log-rank test (Cutoff Finder (Budczies J. *et al.,* 2012)).

Indicators	Category	*p* value	HR	95% CI
Sex	male	0.6481	0.84	0.40–1.77
Age	> 70 years	0.4480	1.33	0.64–2.77
G	G3 (versus G2)	0.2312	1.60	0.74–3.46
pT	pT4 (versus pT2-3)	0.9151	1.05	0.45–2.46
pN	pN1-2 (versus pN0)	0.9683	0.98	0.45–2.18
M	M1 (versus M0)	0.0978	3.41	0.80–14.60
TNM stage	III-IV (versus I-II)	0.8825	1.06	0.49–2.30
LVI	LVI1 (versus LVI0)	0.6737	1.77	0.56–2.43
Pne	Pne1 (versus Pne0)	0.2648	1.67	0.68–4.12
Tumor growth pattern	Infiltrative	0.0075	2.81	1.32–5.98
Tumor budding	High	0.0556	2.05	0.98–4.29
Peritumoral lymphocytes	High	0.5234	1.28	0.61–2.69
Primary tumor localization	Right colon Transverse colon Multiple sites	0.1128	2.00	0.85–4.68
MSI status	MSI	0.0614	2.07	0.97–4.43
BRAF gene	Mutant	0.9501	0.98	0.44–2.18
KRAS gene	Mutant	0.5369	0.78	0.36–1.72
PIK3CA gene	Mutant	0.3264	0.59	0.21–1.70
CD8_CM_d	high, when cf = -0.355	0.0013[*]	0.31	0.15–0.66
CD8_d_S	high, when cf = 5.914	0.3600	1.46	0.64–3.31
CD8_d_TE	high, when cf = 4.963	0.2400	0.64	0.31–1.35
CD8_d_T	high, when cf = 4.059	0.0850	0.53	0.25–1.10
CD8_d_INT	high, when cf = 5.615	0.0670	2.13	0.93–4.88
CD20_CM_d	high, when cf = -0.552	0.0230[*]	0.39	0.16–0.91
CD20_d_S	high, when cf = 2.358	0.0061[*]	0.30	0.12–0.75
CD20_d_TE	high, when cf = 3.684	0.0530	0.33	0.10–1.08
CD20_d_T	high, when cf = 1.219	0.0210[*]	0.43	0.20–0.90
CD20_d_INT	high, when cf = 1.791	0.0230[*]	0.41	0.18–0.90
CD68_CM_d	high, when cf = -0.173	0.1300	1.77	0.84–3.74
CD68_d_S	high, when cf = 5.137	0.1500	0.59	0.28–1.23
CD68_d_TE	high, when cf = 4.524	0.2800	0.65	0.30–1.43
CD68_d_T	high, when cf = 4.018	0.1600	1.82	0.77–4.26
CD68_d_INT	high, when cf = 4.015	0.1700	1.73	0.79–3.81

Multiple Cox regression revealed 3 independent prognostic factors (Table 10): high CM for CD8+ T cell density (CD8 Immunogradient) and high CM for CD20 + B cell density (CD20 Immunogradient); both predicted a 3-3.2-fold longer patient OS, whereas the infiltrative tumor growth pattern was associated with an almost threefold higher risk of death (Model 5, LR: 23.03, p < 0.0001). Additionally, Cox regression model with CM for CD8+ T cell and CD20+ B cell densities only was generated (Model 6, LR: 15.50, p < 0.0001).

Table 10. Multivariate Cox regression models for patient OS; 2nd CRC patient cohort. n = 87.

| Model 5 LR: 23.03, p < 0.0001	χ^2	*p* value	HR	95% CI
CD8_CM_d (high)	8.87	0.0029	0.31	0.14-0.67
CD20_CM_d (high)	6.42	0.0113	0.33	0.14-0.78
Tumor growth pattern (infiltrative margin)	7.24	0.0071	2.90	1.34-6.29
Model 6 LR: 15.50, p = 0.0004	χ^2	*p* value	HR	95% CI
CD8_CM_d (high)	9.61	0.0019	0.30	0.14-0.64
CD20_CM_d (high)	5.18	0.0228	0.37	0.16-0.87

The CD8 Immunogradient in the CRC patient cohort stratified patients into prognostic groups with 75% and 43%, in the MSS tumor subgroup – with 94% and 43%, and in the MSI tumor subgroup – with 65% and 31% 5-year OS probabilities (Figure 10, A-C). CD20 Immunogradient in the CRC patient cohort stratified patients into prognostic groups with 76% and 56%, in the MSI tumor subgroup – with 80% and 40% 5-year OS probabilities (Figure 11, A and C). In the MSS tumors, a high CD20 Immunogradient showed a trend of worse prognosis; however, this result is not statistically reliable (Figure 11, B). According to the tumor growth pattern, tumors with a pushing or infiltrative margin in the CRC patient cohort were associated with 73% and 47%, and in the MSS tumor subgroup – with 89% and 50% 5-year OS probabilities, respectively (Figure 12, A and B); in MSI tumors, the trend of patient stratification by tumor growth pattern was similar but not statistically significant (Figure 12, C)
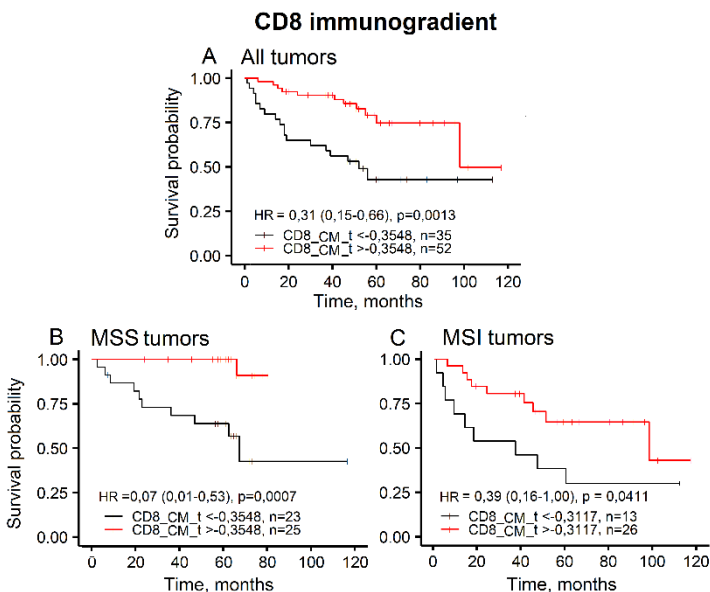
Figure 10. Kaplan-Meier survival curves for overall patient survival obtained by CD8 immunogradient in all tumors (A) and in MSS (B) or MSI tumor (C) subgroups.
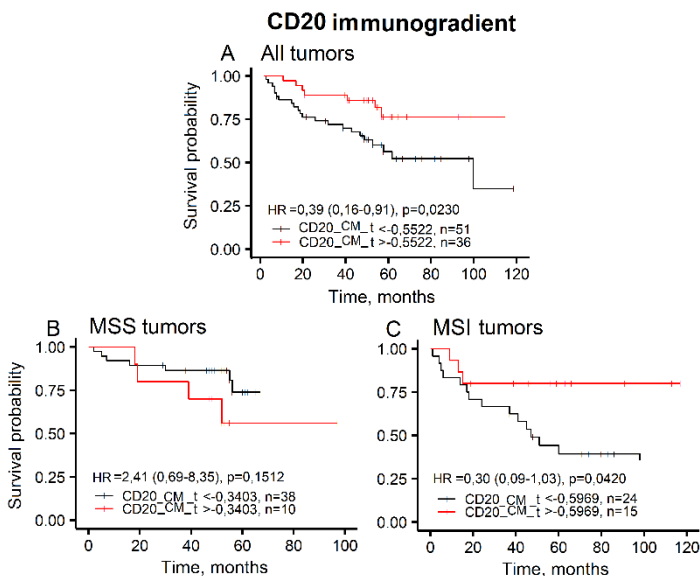
Figure 11. Kaplan-Meier survival curves for overall patient survival obtained by CD20 immunogradient in all tumors (A) and in MSS (B) or MSI tumor (C) subgroups.
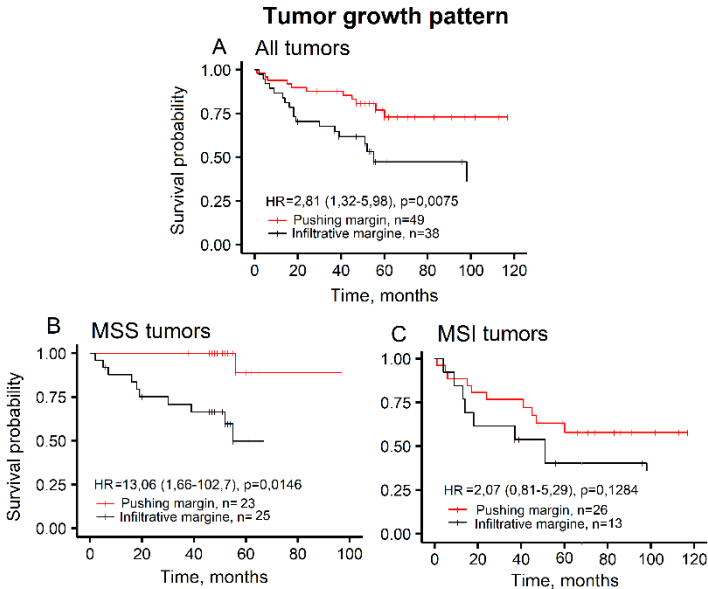
Figure 12. Kaplan-Meier survival curves for overall patient survival obtained by tumor growth pattern in all tumors (A) and in MSS (B) or MSI tumor (C) subgroups.

### 2.3.5. Combined prognostic scores

To integrate the informative value of all 3 independent indicators, we calculated the combined scores:

1) The CD8–CD20 Immunogradient score, which combines IHC marker-based CD8 an CD20 Immunogradients;

2) The immuno-interface score, which combines IHC marker-based CD8 and CD20 Immunogradients with the histological tumor growth pattern feature.

These scores are calculated by summing positive prognostic scores obtained from the patient stratifications based on cut-off values for each factor: high / low CD8 and CD20 Immunogradient estimates were assigned a value of 1 (favourable) / 0 (unfavourable), respectively; pushing /infiltrative tumor growth patterns were assigned a value of 1 (favourable) / 0 (unfavourable), respectively.

The resulting scores stratified patients into 3 and 4 prognostic risk groups (Figure 13).
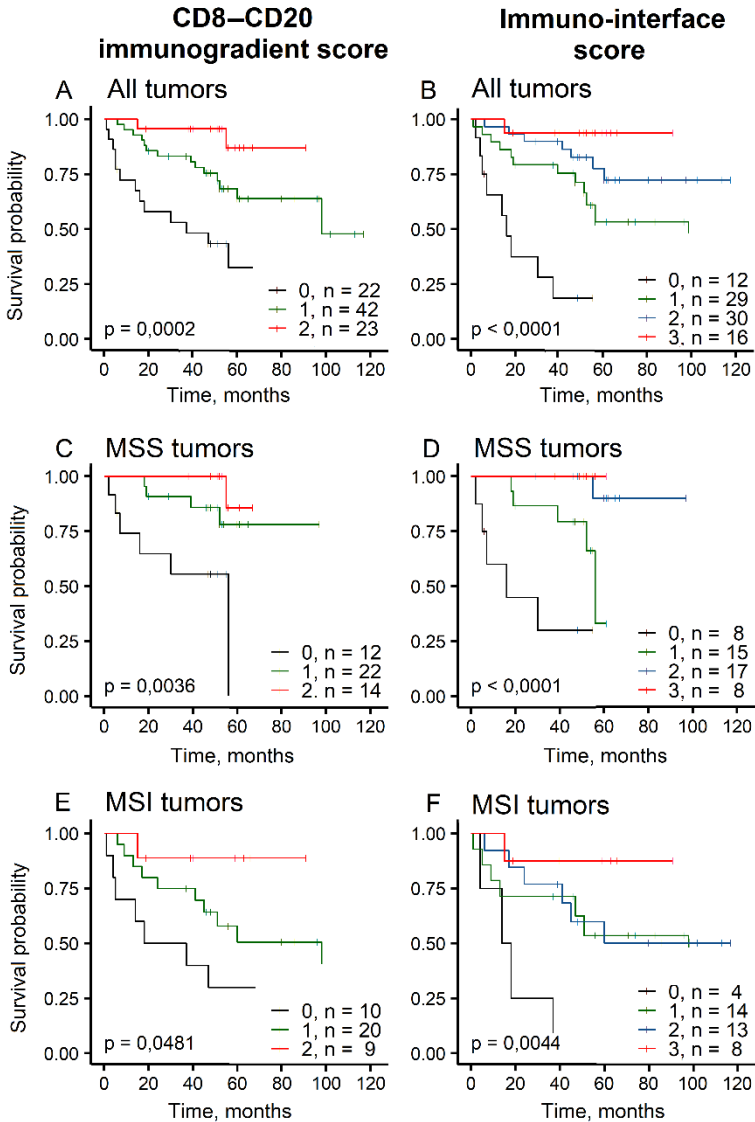
Figure 13. Kaplan-Meier survival curves for patient overall survival obtained by combined scores in all tumors and MSS or MSI tumor subgroups, respectively: A, C, E – CD8–CD20 Immunogradient score; B, D, F – immuno-interface score.

41

CD8–CD20 Immunogradient score stratified patients into 3 groups: score 2 predicted 87%, score 1 – 64%, and score 0 – 33% 5-year OS probabilities (Figure 13, A). The CD8–CD20 Immunogradient score stratified patients into prognostic groups regardless of tumor MSI status: it identified prognostic groups with 86%, 78%, and ~ 50% 5-year OS probabilities in the MSS tumor subgroup, and prognostic groups with 89%, 51%, and 30% 5-year OS probabilities in the MSI tumor subgroup (Figure 13, C and E).

The immuno-interface score stratified patients into 4 prognostic groups: score 3 predicted 94%, score 2 – 73%, score 1 – 53%, and score 0 – 19% 5-year OS probabilities (Figure 13, B). The immuno-interface score stratified patients with a 0–30% 3-year OS probability in the MSS and MSI tumor subgroups (Figure 11, D and F). It suggests that integrating the histological tumor growth pattern feature into the prognostic score enables the identification of patients with the lowest survival probability, regardless of the tumor MSI status.

CONCLUSIONS

1. A novel digital pathology methodology based on DIA data processing using spatial hexagonal grid analytics has been developed for the immune response assessment in the TME. The algorithm detects the tumor-stroma interface zone and quantifies the absolute TIL density and the TIL density gradient (immunogradient) towards the tumor, measured by the Center of Mass and Immunodrop indicators.

2. The prognostic value of the immune response indicators was assessed in two independent cohorts:

   2.1. In the Vilnius patient cohort, the CD8 Immunogradient had the strongest independent value in overall survival predictions in the context of patient age and primary tumor invasion, and outperformed the absolute TIL densities in the TME.

   2.2. In the Nottingham patient cohort, the CD8 Immunogradient and CD20 Immunogradient were independent prognostic factors. Among all clinicopathological and molecular markers tested, the histological tumor growth pattern was the only criterion with an independent value and strengthened the prognostic model. These factors outperformed absolute TIL densities and CD68 Immunogradient in the TME.

3. In the Nottingham patient cohort, combined independent prognostic scores were generated: 1) the CD8-CD20 Immunogradient score based on the CD8 and CD20 IHC markers, which allowed the stratification of CRC patients into 3 prognostic groups, regardless of tumor MSI status; 2) the immuno-interface score based on three indicators (CD8 and CD20 Immunogradients and histological tumor growth pattern) allowed the stratification of CRC patients into 4 prognostic groups and the identification of patients at highest risk of death, regardless of tumor MSI status.

PRACTICAL RECOMMENDATIONS

1. In order to implement IZ Immunogradient-based prognostic models into clinical practice, their value must be confirmed in larger CRC patient cohorts.
2. It is recommended to include IZ Immunogradient indicators in studies of the TME as possible prognostic (predictive) immune response indicators in other cancer types.

PUBLICATIONS AND PRESENTATIONS

Research articles published in journals with a citation index (IF) in the *Clarivate Analytics Web of Science* platform:

Publications directly related to the topic of doctoral dissertation:

1. Rasmusson A, Zilenaite D, **Nestarenkaitė A**, Augulis R, Laurinaviciene A, Ostapenko V, Poskus T, Laurinavicius A. Immunogradient Indicators for Antitumor Response Assessment by Automated Tumor-Stroma Interface Zone Detection. *Am J Pathol,* 2020; 190(6):1309-1322. [IF$_{2019}$ 3.49, Q1]

2. **Nestarenkaitė A**, Fadhil W, Rasmusson A, Susanti S, Hadjimichael E, Laurinaviciene A, Ilyas M, Laurinavicius A. Immuno-Interface Score to Predict Outcome in Colorectal Cancer Independent of Microsatellite Instability Status. *Cancers (Basel)*, 2020; 12(10). [IF$_{2019}$ 6.13, Q1]

Publication not directly related to the topic of doctoral dissertation:

1. Susanti S, Fadhil W, Ebili HO, Asiri A, **Nestarenkaitė A**, Hadjimichael E, Ham-Karim HA, Field J, Stafford K, Matharoo-Ball B, Hassall JC, Sharif A, Oniscu A, Ilyas M. N_LyST: a simple and rapid screening test for Lynch syndrome. *J Clin Pathol*. 2018;71(8):713-720. [IF$_{2017}$ 2.89, Q2]

Oral and poster presentations directly related to the topic of doctoral dissertation at scientific conferences:

Oral and poster presentation:

1. **Nestarenkaitė A**, Rasmusson A, Zilenaite D, Augulis R, Laurinaviciene A, Ostapenko V, Poskus T, Laurinavicius A. Prognostic value of CD8 Immunogradient indicators in tumor-

stroma interface zone of colorectal cancer. 31st European Congress of Pathology, 2019, Nice, France. *Virchows Archiv*, Heidelberg: Springer, ISSN 0945-6317, eISSN 1432-2307, 2019, vol. 475, suppl. 1, p. 206-207.

Poster presentations:

1. **Nestarenkaitė A**, Rasmusson A, Zilenaite D, Augulis R, Laurinaviciene A, Ostapenko V, Poskus T, Laurinavicius A. Prognostic value of CD8 Immunogradient indicators in tumor-stroma interface zone of colorectal cancer. 25th Global Meet on Cancer Research and Oncology, 2019, Rome, Italy.

2. Zilenaite D, Rasmusson A, **Nestarenkaitė A**, Augulis R, Laurinaviciene A, Ostapenko V, Poskus T, Laurinavicius A. The Immunogradient of CD8+ cell density in the tumor-stroma interface zone predicts overall survival of patients with hormone receptor-positive invasive ductal breast carcinoma. 25th Global Meet on Cancer Research and Oncology, 2019, Rome, Italy.

3. Zilenaite D, Rasmusson A, **Nestarenkaitė A**, Augulis R, Laurinaviciene A, Ostapenko V, Poskus T, Laurinavicius A. The Immunogradient of CD8+ cell density in the tumor-stroma interface zone predicts overall survival of patients with hormone receptor-positive invasive ductal breast carcinoma. 31st European Congress of Pathology, 2019, Nice, France. *Virchows Archiv*, Heidelberg: Springer, ISSN 0945-6317, eISSN 1432-2307, 2019, vol. 475, suppl. 1, p. 80-81.

Patent application:

1. Laurinavicius A, Rasmusson A, Zilenaite D, **Nestarenkaitė A**, Augulis R are co-authors of "Automated Tumor-Stroma Interface Zone Detection for Anti-Tumor Response Assessment by Immunogradient Indicators," submitted by Vilnius University for

Lithuanian (LT2019 509) and international (No. PCT/IB2020/053396. International Bureau of the World Intellectual Property Organization) patents for Immunogradient indicators.

Secondment:

1. Secondment (2 months; 2017) at NHS QMC Molecular pathology department (Nottingham, UK) implementing activities under the Marie Skłodowska-Curie Action Program (IAPP Marie Curie Action EU Framework Program AIDPATH: Academia and Industry Collaboration for Digital Pathology).

SUMMARY IN LITHUANIAN

Mokslinis aktualumas ir naujumas

Šiandien esamų naviko histopatologinių ir molekulinių žymenų nepakanka SŽV kliniškai klasifikuoti. Papildomos prognozinės informacijos gali suteikti naviko mikroaplinkos žymenys, ypač NIL, kurie atspindi paciento imuninį atsaką į naviką. Taikant skaitmeninės patologijos metodus, *in situ* imuninio atsako analize įrodyta, kad NIL tankis ir erdvinis pasiskirstymas naviko mikroaplinkoje koreliuoja su pacientų išgyvenamumu ir atsaku į imunoterapijas. Įprastai šie metodai yra pagrįsti NIL tankio skirtinguose naviko mikroaplinkos regionuose ir (arba) atstumų tarp imuninių ir navikinių ląstelių kiekybiniu vertinimu. Nauji skaitmeninės patologijos įrankiai leidžia integruoti įvairius imuninio konteksto aspektus, tačiau, galima teigti, kad erdvinės analitikos galimybės vis dar nėra išnaudotos ieškant prognozinių imuninio atsako rodiklių.

Rašant disertaciją, ieškota skaitmeninės vaizdo analizės ir erdvinės analitikos metodų, kuriais būtų galima nustatyti informatyvius imuninio atsako naviko mikroaplinkoje rodiklius, turinčius savarankišką prognozinę vertę SŽV sergančių pacientų imtyse. Derinant skaitmeninės vaizdo analizės ir dirbtinio intelekto įrankius bei šešiakampių gardelių analitikos principus, taikant unikalių vienareikšmiškai apibrėžtų matematinių taisyklių seką, sukurta metodika, kuria nustatomi naujo tipo rodikliai, pagrįsti NIL tankių profiliais naviko ir stromos sąveikos zonoje. Ši metodika: 1) taiko erdvinės analitikos metodus, skirtus sąveikos zonai tarp navikinio epitelio ir aplinkinės stromos audinio automatiškai nustatyti ir jai suskirstyti; 2) matuoja absoliutų NIL tankį ir jo kryptingą pokytį (imunogradientą) naviko srities link sąveikos zonoje; 3) nustato sąveikos zonos imunogradientu pagrįstus kombinuotus įverčius, kurie yra stiprūs nepriklausomi prognoziniai veiksniai SŽV sergančių pacientų imtyse.

Kitos imuninio atsako profiliavimo metodikos yra pagrįstos NIL tankiais, matuojamais naviko šerdyje ir IK (Pages F *et al.*, 2018), tačiau nevertina kryptingo NIL tankio profilio navikinio epitelio ir aplinkinės stromos sąveikos regionuose. Be to, šios metodikos įprastai naudoja fiksuoto pločio IK, kuris dėl dažnai netolygaus, infiltruojančio naviko augimo pobūdžio gali sukelti matavimų paklaidų. Priešingai, sąveikos zonos samprata ir metodas yra pagrįsti tam tikros naviko mikroaplinkos vietos, kuri apima naviko kraštą (NK) ir sąveikos zonos sritis link naviko ir stromos, tikimybe. Šis metodas grindžiamas vienareikšmiškai apibrėžtomis taisyklėmis ir leidžia pritaikyti kintančio pločio sąveikos zoną, kuri labiau atitinka navikinio audinio erdvinę įvairovę. Sąveikos zona gali būti pritaikyta įvairių imuninių infiltratų skirtinguose audiniuose tyrimams. Sąveikos zona ir joje matuojami imuninio atsako rodikliai yra pagrįsti didelio pajėgumo ir automatizuotomis kompiuterinėmis procedūromis, todėl nepriklauso nuo ekspertinio vizualaus vertinimo ir dažnai atspindi subvizualius požymius, kurių negalima vertinti įprastiniais mikroskopijos metodais.

Disertacijoje siūlomi nauji imuninio atsako rodikliai. Jų prognozinė vertė tirta dviejose SŽV sergančių pacientų, gydytų Vilniaus ir Notingamo (Jungtinė Karalystė) sveikatos priežiūros institucijose, imtyse. Citotoksinių T ląstelių (CD8) imunogradientas (abiejose imtyse), B ląstelių (CD20) imunogradientas ir histologinis naviko augimo pobūdis (Notingame gydytų pacientų imtyje) buvo nepriklausomi prognoziniai pacientų bendrojo išgyvenamumo veiksniai. CD8 ir CD20 imunogradientai pranoko absoliutaus NIL tankio naviko mikroaplinkoje rodiklius ir standartinius klinikinius, patologinius ir molekulinius žymenis.

Sudaryti nauji kombinuoti modeliai pacientų bendrajam išgyvenamumui prognozuoti: CD8–CD20 imunogradiento įvertis, pagrįstas tik CD8 ir CD20 IHC žymenimis, ir imuninės sąveikos įvertis, kuris papildomai integruoja histologinį naviko augimo pobūdžio kriterijų. Šie įverčiai prognozine galia pranoko navikų TNM kriterijus ir MSI požymius, kurie iki šiol yra vieni pagrindinių

rodiklių, numatant SŽV klinikinę eigą ir atsaką, skiriant citotoksinę chemoterapiją ar imunoterapiją.

Darbo tikslas ir uždaviniai

Šio **darbo tikslas** – sukurti kiekybinę ir automatizuotą skaitmenine vaizdo analize pagrįstą imuninio atsako vėžio mikroaplinkoje matavimo sistemą ir įvertinti jos prognozinę galią storosios žarnos vėžiu sergančių pacientų imtyse.

Iškelti **darbo uždaviniai:**
1. Sukurti skaitmenine mikroskopinio vaizdo analize ir erdvine statistika pagrįstą metodiką, skirtą imuninių ląstelių pasiskirstymui naviko mikroaplinkoje profiliuoti, ir informatyvius kiekybinius rodiklius imuniniam atsakui storosios žarnos vėžio mikroaplinkoje matuoti.
2. Įvertinti imuninio atsako rodiklių prognozinę vertę dviejose nepriklausomose storosios žarnos vėžiu sergančių pacientų imtyse.
3. Sudaryti kombinuotus prognozinius modelius, taikytinus esant storosios žarnos vėžiui, ir nustatyti jų vertę, siejant su standartiniais klinikiniais, patologiniais ir molekuliniais rodikliais.

Ginamieji disertacijos teiginiai

1. Naviko ir stromos sąveikos zonos imunogradiento rodikliais įvertinti NIL yra nepriklausomi prognoziniai SŽV sergančių pacientų bendrojo išgyvenamumo veiksniai, informatyvesni negu absoliutus NIL tankis naviko mikroaplinkoje ir standartiniai klinikiniai, patologiniai ir molekuliniai rodikliai.
2. Kombinuoti CD8–CD20 imunogradiento ir imuninės sąveikos įverčiai yra stiprūs nepriklausomi prognoziniai SŽV sergančių pacientų bendrojo išgyvenamumo veiksniai, pranokstantys navikų TNM kriterijus ir MSI požymius.

IŠVADOS

1. Imuniniam atsakui vėžio mikroaplinkoje vertinti sukurta skaitmeninės patologijos metodika, pagrįsta vaizdo analizės duomenų apdorojimu erdvinės šešiakampių gardelių analitikos principais. Šia metodika automatizuotai nustatoma naviko ir stromos sąveikos zona ir joje kiekybiškai įvertinamas imuninių ląstelių absoliutus tankis bei tankio gradientas (imunogradientas) link naviko, matuojamas masės centro ir imunonuokryčio rodikliais.

2. Imuninio atsako rodiklių prognozinė vertė įvertinta dviejose nepriklausomose SŽV sergančių pacientų imtyse:

   2.1. Vilniaus pacientų imtyje, prognozuojant bendrąjį išgyvenamumą, CD8 imunogradientas turėjo stipriausią nepriklausomą vertę pacientų amžiaus bei pirminio naviko išplitimo kontekste ir pranoko absoliutaus NIL tankio naviko mikroaplinkoje rodiklius.

   2.2. Notingamo pacientų imtyje, prognozuojant bendrąjį išgyvenamumą, CD8 imunogradientas ir CD20 imunogradientas buvo nepriklausomi veiksniai. Iš visų tirtų klinikinių, patologinių ir molekulinių rodiklių histologinis naviko augimo pobūdis buvo vienintelis kriterijus, kuris turėjo nepriklausomą vertę ir sustiprino prognozinį modelį. Minėti veiksniai pranoko absoliutaus NIL tankio ir CD68 imunogradiento naviko mikroaplinkoje rodiklius.

3. Notingamo pacientų imtyje sudaryti kombinuoti nepriklausomi įverčiai: 1) CD8–CD20 imunogradiento įvertis, pagrįstas tik CD8 ir CD20 IHC žymenimis, leidžia patikimai stratifikuoti SŽV sergančius pacientus į 3 prognozines grupes, nepriklausomai nuo naviko MSI požymių; 2) imuninės sąveikos įvertis, pagrįstas trimis rodikliais (CD8 ir CD20 imunogradientais ir histologiniu naviko augimo pobūdžiu), leidžia patikimai stratifikuoti SŽV sergančius pacientus į 4 prognozines grupes ir, nepriklausomai nuo naviko MSI požymių, išskirti pacientus, kuriems kyla didžiausia mirties rizika.

PRAKTINĖS REKOMENDACIJOS

1. Į klinikinę praktiką siekiant įdiegti naviko ir stromos sąveikos zonos imunogradientu pagrįstus prognozinius modelius, jų vertė turi būti patvirtinta didesnėse SŽV sergančių pacientų imtyse.
2. Naviko ir stromos sąveikos zonos imunogradiento rodiklius rekomenduojama įtraukti į naviko mikroaplinkos tyrimus kaip galimus prognozinius (predikcinius) imuninio atsako rodiklius esant ir kitoms vėžio atmainoms.

CURRICULUM VITAE

Name and surname:		Aušrinė Nestarenkaitė
Date of birth:		October 7, 1988
Contacts:		Phone No. +370 604 40 690
		Email:
		ausrine.nestarenkaite@vpc.lt

Education:	2007–2011	Bachelor in Bioengineering, Faculty of Fundamental Sciences, Vilnius Gediminas Technical University, Vilnius, Lithuania
	2011–2013	Master in Genetics, Faculty of Natural Sciences (now – Life Sciences Center), Vilnius University, Vilnius, Lithuania
	2012–2013	Molecular biology studies (Erasmus student exchange program), Faculty of Natural Sciences, Aarhus University, Aarhus, Denmark
	2015–present	Doctoral studies in Biomedical Sciences, Institute of Biosciences, Life Sciences Center, Vilnius University, Vilnius, Lithuania

Employment:	2014–present	Medical geneticist at the National Center of Pathology, Affiliate of Vilnius University Hospital Santaros Klinikos, Vilnius, Lithuania

NOTES

NOTES